Characterization of the cutting phenomenon in orbital drilling of titanium alloys (TiAl6V4)

P. A. Rey, Johanna Senatore, Yann Landon

HSM2014-00000

CHARACTERIZATION OF THE CUTTING PHENOMENON IN ORBITAL DRILLING OF TITANIUM ALLOYS (TIAL6V4)

P.A .Rey, K .Moussaoui, J. Senatore, Y. Landon

Institut Clément Ader (ICA) Université de Toulouse ; INSA, UPS, Mines Albi, ISAE

Bât 3R1, 118 route de Narbonne, F-31062 Toulouse Cedex 9, France.

*P.A. Rey; pierre-andre.rey@univ-tlse3.fr

Abstract

The orbital drilling is a complex operation. Due to the tool trajectory, which is helical, chip thickness is highly variable. This is why the cutting forces are very difficult to estimate.

The aim of this study is to determinate influence of tool geometry and cutting conditions on cutting force and to determinate the final quality of the machined hole. At first, the geometry of the chip is modeled taking into account the parameters defining the trajectory and the tool. A cutting force model based on the instantaneous chip thickness is then set up. An experimental part validates the cutting force model through measures of cutting force made during orbital drilling tests. Another experimental part is made. A series of drilling by varying the geometry of the tool is realized. During all these drillings, cutting forces will record using the Kistler dynamometer. And then a dimensional measure will be realized on all holes using a three-dimensional measuring machine.

Using cutting force model and the results of tests, it is possible to conclude on the influence of the tool geometry, on the hole geometry. And so it's possible to optimize these parameters in order to increase the final quality of the hole.

Keywords:
Orbital drilling, TiAl6V4, tool geometry, cutting forces,

1 INTRODUCTION

The orbital drilling, also called helical milling, is a process notably used in the aeronautical industry. It is very different from the axial drilling. It consists in machining a hole with a tool which has a smaller diameter, driven on a helical trajectory (Figure 1).
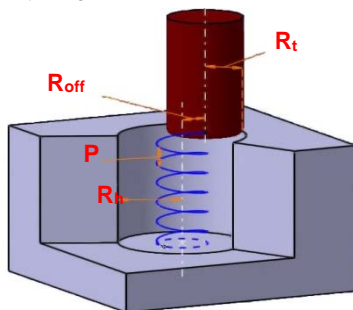

Figure 1 Orbital drilling's trajectory

This process is used especially because it generates low cutting forces [Lutze, 2008]. As a consequence, the burr formation at the entry and at the exit of the hole is largely reduced, and also the risk of delamination when drilling composite materials is highly reduced. [Denkena and al.,

2008] [Brinksmeier et al., 2008]. Operations such as cleaning or deburring are then considerably reduced.

For the cutting force model in orbital drilling, three approaches are possible: the numerical approach, the analytical and the semi analytical approach. The numerical approach used in the work of Lorong [Lorong et al, 2002] aims to simulate chip formation by a finite element study. Analytics approaches as Merchant's model Merchant, 1945] or Oxley's model [Oxley, 1989] consist to describe the most physically possible the cutting phenomenon in order to calculate the cutting forces. The semi-analytics approaches, also called mechanistic approaches, are the most used one to calculate machining cutting forces and particularly when the process is complex [Fontaine, 2004], like helical milling. This approach is based on analytics approaches by simplifying all the parameters of the tool geometry or of the tool/workpiece couple by a constant experimentally defined with calibration test.

2 MODELING OF ORBITAL DRILLING

2.1 Geometrics settings of the orbital drilling

In order to be able to develop a model of the chip geometry, the input data of the model and the references that are necessary to form the equation, need to be previously defined.

The defining data of the tool's geometry:

The global tool geometry (Figure 2) is generically defined using the following parameters:

- Tool outside radius: Rt
- Number of tooth: Z
- Number of tooth with center cut: Zcc
- Corner radius: Rb
- Radius without center cut: Rcc
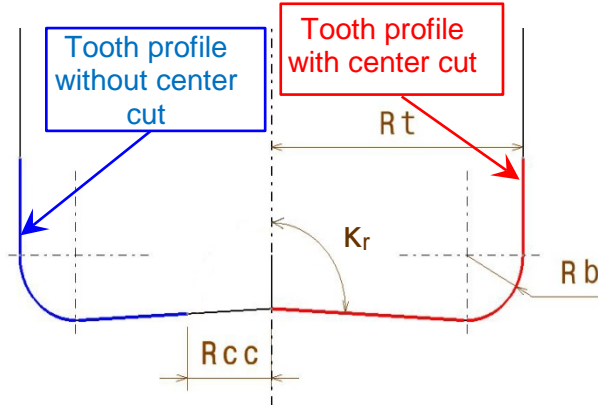- Tool cutting edge angle: κr

Figure 2 : Tool geometry

Cutting's parameters:

In order to determine the chip thickness, it is necessary to define the cutting parameters. The tool feed, along helical trajectory, can be decomposed in an axial feed fa and a tangential feed ft.

Drilling radius: Rh

Interpolation radius, called offset: Roff= Rh – Rt

Pitch (mm): P

Cutting speed (m/min): Vc

Axial feed (mm/rev): fa

Tangential feed (mm/rev): ft

Axial feed per tooth: f_za=f_a/Z

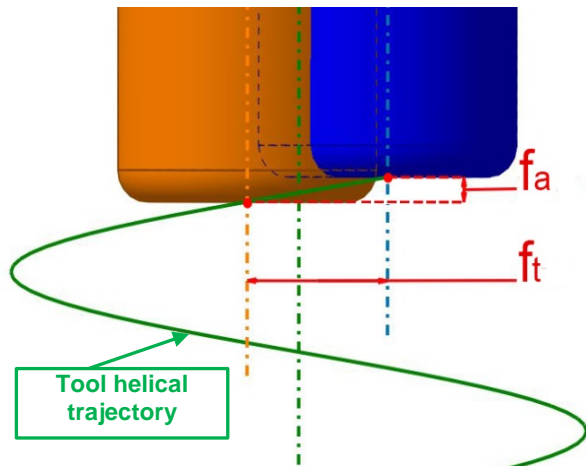Tangential feed per tooth: f_zt=f_t/Z

Figure 3 : Feed definition.

References definition:

Hole center to drill: HL

Machine's reference: this reference is fixed.

$$R_m = (HL, X, Y, Z)$$

Orbital reference: this reference permit to define the tool's positions « i » on the helical trajectory.

$$R_{oi} = (HL, X_{oi}, Y_{oi}, Z)$$

With: $\begin{vmatrix} X_{oi} = \cos\theta_i . X + \sin\theta_i . Y \\ Y_{oi} = -\sin\theta_i . X + \cos\theta_i . Y \end{vmatrix}$

The angle θ_i defines the tool angular position considered in the machine reference. The tool center position in position « i » is called CL_i, at a distance R_{off} to HL.

Tool reference: This reference can get the location of every points of the tool « i » in the orbital reference.

$$R_t = (CL_i, X_{ci}, Y_{ci}, Z)$$

With: $\begin{vmatrix} X_{ci} = \cos\varphi_i . X_{oi} + \sin\varphi_i . Y_{oi} \\ Y_{ci} = -\sin\varphi_i . X_{oi} + \cos\varphi_i . Y_{oi} \end{vmatrix}$

The angle φ_i defines the angular position of considerate point of the tool in the orbital reference
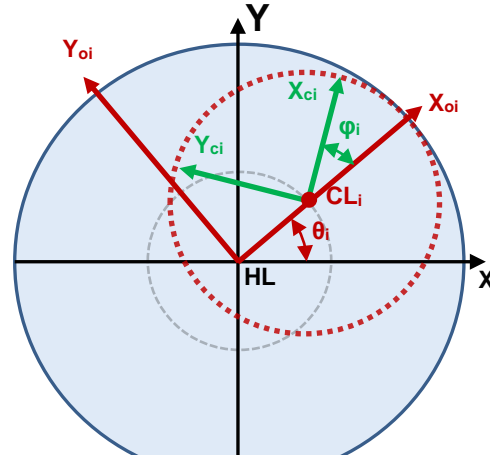

Figure 4 References definition

Representative function of cutting edge profile

In order to calculate the chips section, it's necessary to define the cutting edge profile. The function *Hk(r)* is established, to give the elevation of each cutting edge point versus radius *r*. The lowest tool point « k » is defined at the elevation Z = 0. This function is decomposed into several successive functions, to take into consideration the different tool geometries.

Examples, the evolution of the function *Hk(r)* for a tooth without center cut, is represented Figure 5.

- If $0 < r < R_{cc}$:

$$H_k(r) = d$$

d is a value arbitrarily set to ensure the non-participation of the area during the machining.

- If $R_{cc} < r < R_t - R_b$:

$$H_k(r) = [r - (R_t - R_b)].tan\left(\frac{\pi}{2} - \kappa_r\right)$$

- If $R_t - R_b < r < R_t$:

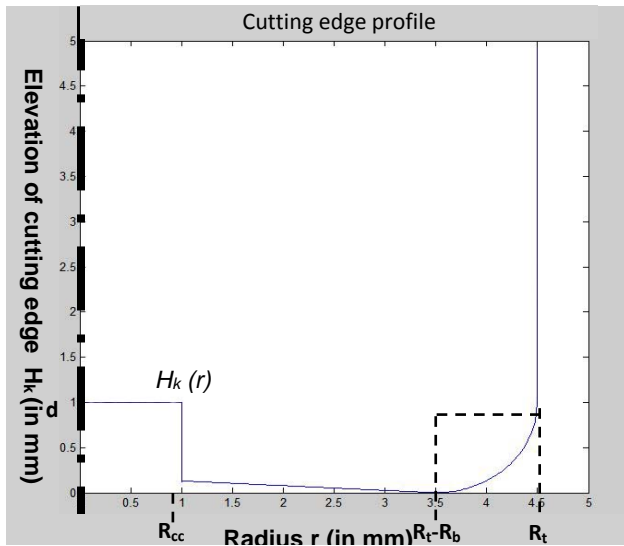$$H_k(r) = R_b - \sqrt{R_b^2 - [r - (R_t - R_b)]^2}$$

Figure 5 : Representation of the cutting edge profile « k » without cutting tool center

Calculation of the machined chip section by a tooth

Hypothesis:

As the cutting speed is largely higher than the tool feed speed, two simplifying hypothesis are made:

- The tooth trajectory is considered circular (cycloid neglected) **[Segonds et al., 2006]**

- The calculation of volume machined by the tool at the present moment is the result of a Boolean subtraction operation between the volume of the machined work piece at the previous moment and the volume envelope of the tool, the tool being positioned on its trajectory.

Therefore, to calculate the chip section machined by a tool tooth « i » at the present time (the tool identified by its tool center's point **CL$_i$**) two calculation steps are made:

First, each point A_i belonging to the envelope surface of the tool « i » is detected in $\boldsymbol{R_{oi}}$ from its coordinates (X_{Ai}, Y_{Ai}, Z_{Ai}) in function of r_{Ai} et φ_i $(r_{Ai}\epsilon[0, R_t], \varphi_i\epsilon[0,2\pi])$, and the function H_k applied at the tool « i » :

$$A_i \begin{cases} X_{Ai}(r_{Ai}, \varphi_i) = r_{Ai}.\cos \varphi_i \\ Y_{Ai}(r_{Ai}, \varphi_i) = r_{Ai}.\sin \varphi_i \\ Z_{Ai}(r_{Ai}, \varphi_i) = H_i(r_{Ai}) \end{cases}$$

The set of the points A_i for a constant φ_i, represent the tooth where the chip section is assessed on.

Then, to identify the surface location previously machined on each point A_i, all the locations of the tool that interve before the location « i » on a complete orbit revolution are considered. It will then be possible to estimate the height of the machined material at the point A_i. Each considered previous location is identified by its tool center point **CL$_k$**.

The difference of altitude following $\boldsymbol{Z}$ between two tool locations **CL$_i$** and **CL$_k$** is called H_{ki}. Knowing that the tool describes a helical trajectory characterized by its pitch P (Figure 3), the height H_{ki} is defined according to the relative angular position of **CL$_i$** and **CL$_k$** on the trajectory characterized by θ_{ki} (*Figure 6*):

$$H_{ki}(\theta_{ki}) = P - \frac{P \times \theta_{ki}}{2 \times \pi}$$

Then, for each tool point A_i considered, the set of the points A_k of which the coordinates in the locator $\boldsymbol{R_{oi}}$ are such that $(X_{Ak} = X_{Ai}, Y_{Ak} = Y_{Ai})$ are identified. The coordinate Z_{Ak} of the point A_k can be calculated through the function H_k :

$$A_k \begin{cases} X_{Ak}(r_{Ai}, \varphi_i) = X_{Ai} \\ Y_{Ak}(r_{Ai}, \varphi_i) = Y_{Ai} \\ Z_{Ak}(r_{Ak}, \theta_{ki}) = H_k(r_{Ak}) + H_{ki}(\theta_{ki}) \end{cases}$$

For this the radius r_{Ak} has to be previously determined. From Figure 6, by considering the triangle(CL_k, A_k, HL) :

$$r_{Ak}(r_{Ai}, \varphi_i, \theta_{ki})$$
$$= \sqrt{\left|r_{ki}^2 + R_{off}^2 - 2 \times R_{off} \times r_{ki} \times \cos(\theta_{ki} - \alpha)\right|}$$

With: $\alpha(r_{Ai}, \varphi_i) = \cos^{-1}\left(\frac{r_{ki}^2 + R_{off}^2 - r_{Ai}^2}{2 \times r_{ki} \times R_{off}}\right)$

And by considering the triangle(A_i, HL, CL_i) :

$$r_{ki}(r_{Ai}, \varphi_i) = \sqrt{\left|r_{Ai}^2 + R_{off}^2 - 2 \times R_{off} \times r_{Ai} \times \cos(\pi - \varphi_i)\right|}$$
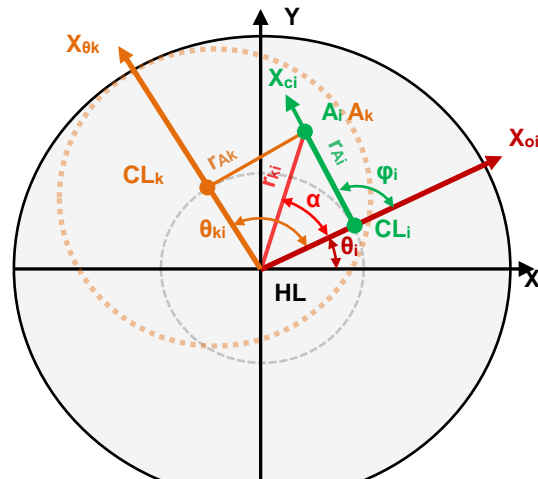

Figure 6 Locating a tool "k" relative to the tool "i"

For each point A_i considered, points A_k for every tool location « k » of the previous orbit revolution are calculated. To determinate the location of the machined surface, the point A_k with the weakest altitude is kept and called S_k.

$$S_k \begin{cases} X_{Sk}(r_{Ai}, \varphi_i) = X_{Ak} \\ Y_{Sk}(r_{Ai}, \varphi_i) = Y_{Ak} \\ Z_{Sk}(r_{Ai}, \varphi_i) = \min_{0 \leq \theta_{ki} \leq 2\pi}(Z_{Ak}) \end{cases}$$

The chip section on a tooth is then obtained by plotting the set of points A_i and the associated points S_k, for a fixed angle φ_i (representing a tooth of the tool) and for $r_{Ai}\epsilon[0, R_t]$ (Figure 7).

This section is then split into trapezoids of thickness h_k and width b_k.

The thickness h_k is the normal distance to the tool profile between the profile A_i and the previously machined surface S_k, it represents the chip thickness.

The width b_k is the distance between points A_i, it is set arbitrarily.
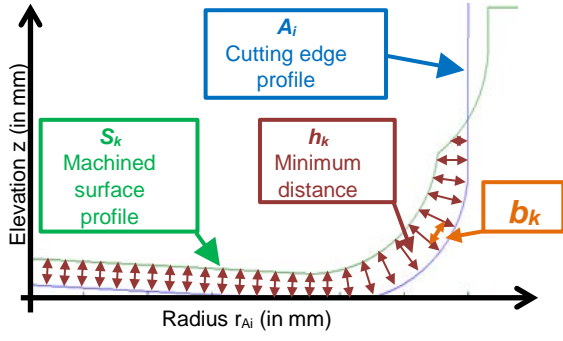
Figure 7 : Decomposition of the chip section

If the decomposition is sufficiently thin (small width b_k compared to the radius of the tool), each trapezoid can be approximated and simplified by a rectangle. The chip section S_c can then be written:

$$S_c(\varphi_i) = \sum_{r_{Ai}=0}^{Rt} b_k(r_{Ai}, \varphi_i) . h_k(r_{Ai}, \varphi_i)$$

Calculation of the cutting force

The chip section in each moment being determined, the forces applied on the tool during drilling can be modeled.

In this article, only the modeling of the cutting force normal to the chip section is presented and discussed. This effort is the most important and is the main cause of tool bending.

The other two components can be modeled in the same way.

The modeling approach is semi-analytical [Merchant, 1945], which gives for the same tool/work piece couple:

$$F_{cut} = K_c \times b \times h$$

Where K_c is a specific cutting coefficient that will remain constant for the first part of the study and will be identified with calibration tests.
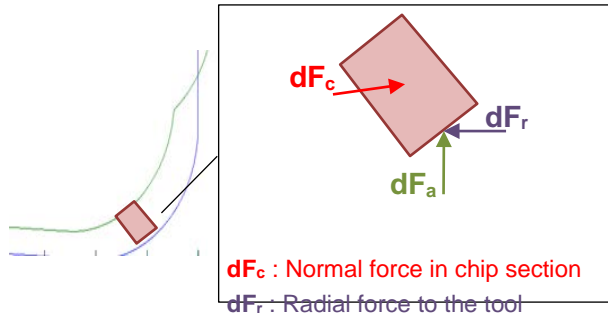

Figure 8 : Forces applied on the tool for a chip section

This model is applied to each trapezoid of the chip section and then summed to obtain the total cutting force when the tooth is in position φ_i.

$$dF_{c\,zi}(r_{Ai}, \varphi_i) = K_c \times b_k(r_{Ai}, \varphi_i) \times h_k(r_{Ai}, \varphi_i)$$

$$F_{c\,zi}(\varphi_i) = \sum_{r_{Ai}=0}^{Rt} dF_c(r_{Ai}, \varphi_i)$$

The evolution of the cutting force of a tooth on a tool revolution is calculated by varying φ_i from 0 to 2π (Figure 9).
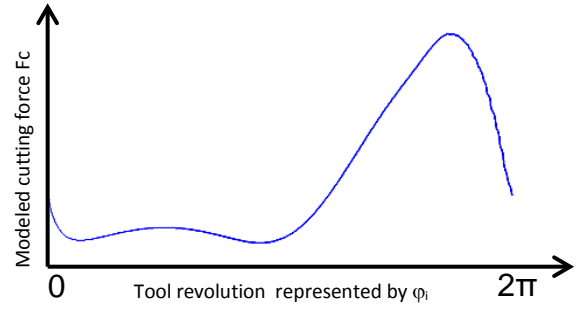

Figure 9 : Evolution of the cutting force for a tooth without the center cut on a tool revolution

This cutting force $F_{c\,zi}(\varphi_i)$ must be calculated for each tooth of the tool, taking into account the differences in the tooth profile which may exist (ex: with or without center cut).
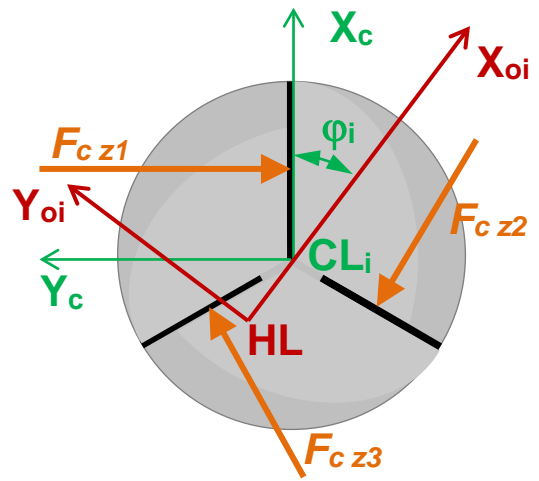

Figure 10 : Representation of cutting forces on a tool with three teeth and with a single tooth with center cut.

To calculate the resulting force, every effort is expressed in the orbital reference R_{oi}, so (Figure 10):

$$\boldsymbol{F_{c\,z1}} \begin{Bmatrix} F_{cut\,z1}(\varphi_i).\sin(\varphi_i) \\ -F_{cut\,z2}(\varphi_i).\cos(\varphi_i). \\ 0 \end{Bmatrix}_{R_{oi}}$$

$$\boldsymbol{F_{c\,z2}} \begin{Bmatrix} F_{cut\,z2}\left(\varphi_i + \dfrac{2\pi}{Z}\right).\sin(\varphi_i + \dfrac{2\pi}{Z}) \\ -F_{cut\,z2}\left(\varphi_i + \dfrac{2\pi}{Z}\right).\cos(\varphi_i + \dfrac{2\pi}{Z}) \\ 0 \end{Bmatrix}_{R_{oi}}$$

$$\boldsymbol{F_{c\,z3}} \begin{Bmatrix} F_{cut\,z3}\left(\varphi_i + \dfrac{4\pi}{Z}\right).\sin(\varphi_i + \dfrac{4\pi}{Z}) \\ -F_{cut\,z3}\left(\varphi_i + \dfrac{4\pi}{Z}\right).\cos(\varphi_i + \dfrac{4\pi}{Z}) \\ 0 \end{Bmatrix}_{R_{oi}}$$

The resulting force $\boldsymbol{F_c}$ is then:

$$\boldsymbol{F_c} = \boldsymbol{F_{c\,z1}} + \boldsymbol{F_{c\,z2}} + \boldsymbol{F_{c\,z3}}$$

3 EXPERIMENTAL PROCEDURES

All tests were performed in a test piece in TiAl6V4 of 19mm thick. The cutting conditions are as follows:

Vc= 30mm/min;

Fza=0.005mm/tooth;

Fzt= 0.04mm/tooth.

The tool used is a tool with three teeth (Z=3) ,with a single tooth with center cut and of diameter D_t = 9mm.

3.1 Identification of specific cutting coefficient

To identify the specific cutting coefficient Kc, tests of slot machining were carried out on a machining center. The force measurement is performed using a Kistler dynamometer. The cutting coefficient, assumed to be constant, can be identified from the measurement of the maximum cutting force. The chip thickness is 0.04mm per tooth, the depth of cut is 0.75mm, and so the maximum chip section is 0.03mm ².

It can be deduced: $Kc = \frac{Fc_{max}}{Sc_{max}}$

Maximum force Fxy observed during the test is 105N. This gives a specific cutting coefficient for our tool/work piece couple of: Kc = 3500N/mm ².

This Kc value is a first approximation for model validation. It doesn't take into account influence of chip thickness or possible influence of speeds. And thereafter, two coefficient will be identified, one for the axial part and one for radial part, because the radial and axial parts present different cutting angles.

3.2 Force measurement in orbital drilling

Tests are also conducted in orbital drilling, in order to have a database to validate the modeling. These tests are performed on a drill bench equipped with an orbital spindle. On all tests, cutting forces are recorded using the dynamometer Kistler and sampled at 10 kHz. On the signals obtained when measuring just a taring is performed.

The hole diameter is 11.1mm and it is made with the same tool which has diameter of 9mm.

Three different geometry tools are tested (Figure 11). Only the axial part is different. The first tool is the tool previously studied with one teeth with cutting tool center and the tool cutting edge angle κr=93°. The second tool is a similar tool, only the tool cutting edge angle is different. The axial part of the second tool is flat so κr=90°. The third is the same than the second without the cutting tool center.

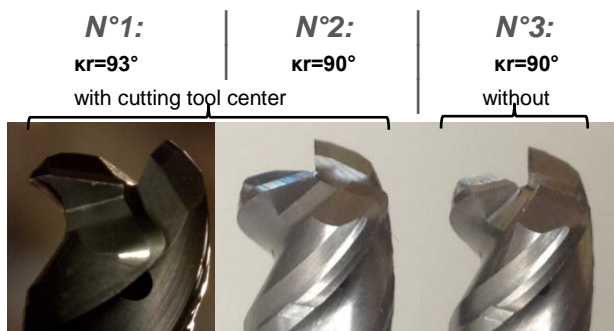| N°1:	N°2:	N°3:
κr=93°	κr=90°	κr=90°
with cutting tool center		without

Figure 11 : The different geometry tool

For comparison of the three tools, cutting conditions have remained the same and are the conditions recommended by the manufacturer: Vc=30m/min; fa=0.013mm/rev; ft=0.12mm/rev.

4 RESULTS AND DISCUSSIONS

The Kistler 9257B dynamometer allows measuring the resultant force in the plane normal to the axis of the tool *Fxy*

With $Fxy = \sqrt{Fx^2 + Fy^2}$ (Figure 11)

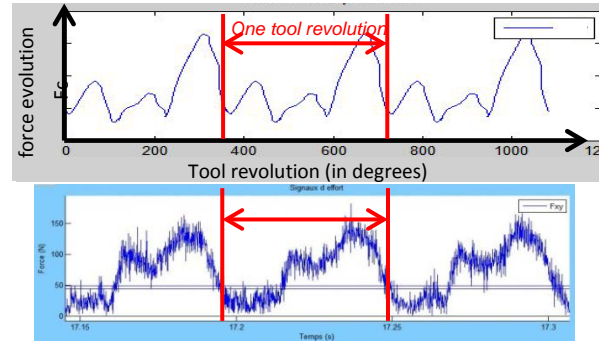The force F_{cT} obtained by modeling differs from the real effort measured Fxy (Figure 11)

Figure 12: Comparison of the evolution of the cutting force over three revolution of tools (modeling at top; measure down for the tool n°1)

The evolution of the modeled force on a tool revolution shows the successive passage of three teeth. This is explained by the fact that the radial chip is not constant on the tool revolution. In addition there is a single tooth with center cut, therefore causing disruption on the tool revolution.

The force measurement Fxy shows only two peaks of effort. Either the force is compensated perfectly on the third revolution, or either the chip is not constant for all three teeth.

This difference between the two graphs is the lack of taking into consideration of cutting phenomena. To improve the model, the tool will be divided into two different parts, in order to better understand how each part works. The axial and radial parts of the tool is defined as (Figure 12).
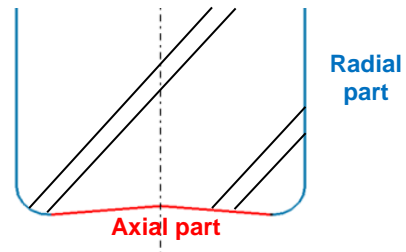

Figure 13: Tool division in two parts

The tool performance and the cutting phenomena caused by the radial part of the tool are known and already considerably studied in the literature. Modeling the cutting force of the axial part is more complex because the tool profile of the tip (Figure 12) combined with the tool trajectory is not classical.

In order to better understand the mechanisms during drilling, the evolution of the tangential force F_t at the contact point tool / work piece (according to **Yoi**) and of the radial force F_r (Figure 14) are modeled.

These two efforts strongly oscillate on a tool revolution, causing a variable bending force of the latter.

So a dynamic phenomenon is established and must be taken into account in the model to adjust the chip thickness of the radial cut. The Figure 14 shows that when the tooth with center cut is located in the "A" area ($0 < \varphi < \frac{\pi}{2}$), the radial force and tangential force are positive but quite low, not causing a significant modification in radial section.

When the tooth with center cut (z_1) is located in the "B" area ($\frac{3\pi}{2} < \varphi < 2\pi$), the radial force and tangential force

are positive. Therefore this resultant force tends to push the tooth being machined towards the surface.

When the tooth with center cut is located in the area "C", the radial force is positive and tangential force is negative. Therefore this resultant force tends to push the tooth (z_2) towards hole surface and in reverse tends to withdraw the tooth (z3) of hole surface.

And when the tooth with center cut is located in the area "D", the radial and tangential force are negatives. Therefore this resultant force tends to withdraw the tooth (z3) of hole
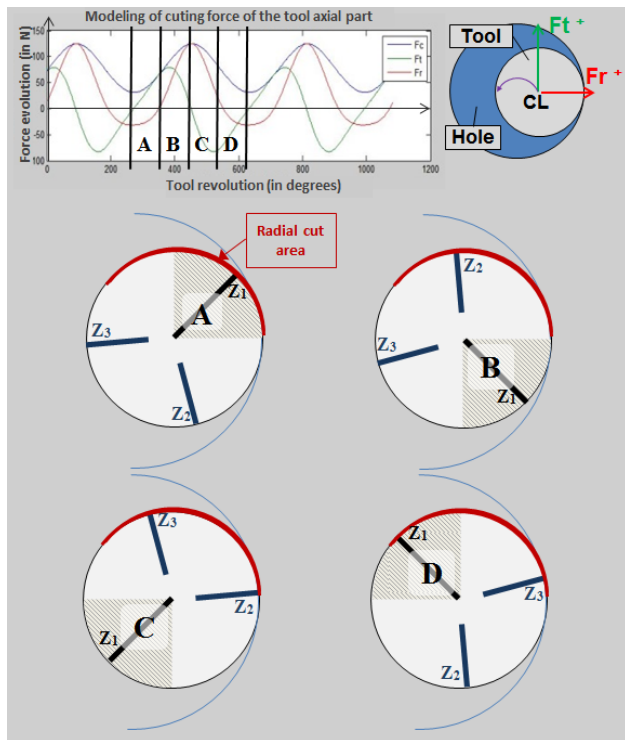

Figure 14 Modeling of the radial and tangential force of the tool axial part, taking into account the three teeth.

The hypothesis is that the radial section isn't homogeneous for the three teeth, because bending forces are different to each passage of various teeth on the radial cut area. The radial chip thickness machined by the tooth z_2 is greater than that machined by the tooth z_3.

In order to bring out this dynamic phenomenon, a series of holes is created with each tool, with the similar conditions (material, cutting parameters, hole diameter) for each tool. And then the diameters of the holes will be measured on the three-dimensional measuring machine (MMT).
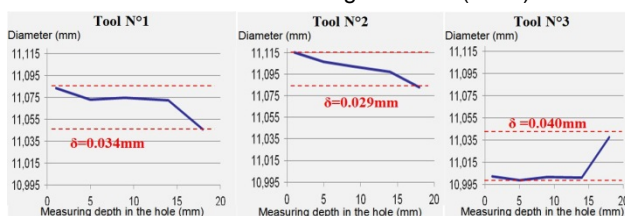

Figure 15 : Average profile measured on the hole for each tool

These measurements show that with same cutting conditions the profile of the hole can be different. And especially that the axial part of the tool is very important on the profile, therefore on the bending tool.

On the profile of the first tool the entrance hole diameter is larger than output. This validates the result of the modeling of the cut (Figure 14) that the cut of the axial part

of the tool causes a positive average radial force, increasing the hole diameter. And at the end of the drilling there is no cutting of the axial part therefore the diameter of the hole decreases.

Between the profile of the first tool and the second, only the tool cutting edge angle is different. The influence of this angle on the axial chip is showed on the Figure 16.
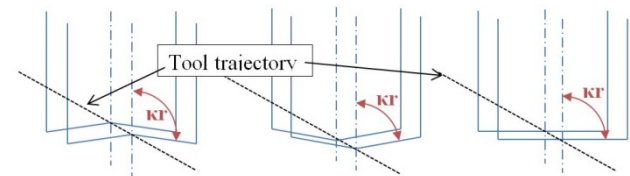

Figure 16 : influence of tool cutting edge angle on the axial chip geometry

Therefore the axial chip for the second tool is more homogeneous, which can be seen also on the modeling effort. The maximum radial force modeled for the second tool is 100N whereas for the first tool it's 150N, it's a reason why the variation of hole diameter is less important for the second tool
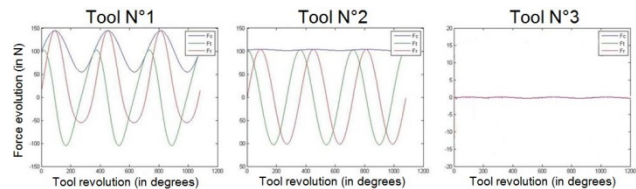

Figure 17 : Modeling of the cutting force of the tool axial part for the three tools

As regards the third tool, the three teeth are identical and the axial part is flat so the chip is identical for the three teeth. That is why the model shows no cutting force because the forces on each tooth cancel each other.

Without the radial force generated by the axial part, the tool during the drilling bend and therefore realized a smaller diameter. The increase of diameter at the end of drilling, is due to the relaxation of the tool.

5 CONCLUSIONS AND PERSPECTIVES

This model, with the integration of the tool geometry, allowed knowing the exact geometry of the chip. With this knowledge, the modeling of the cutting force is possible which allows a better understanding of the cut phenomena when orbital drilling with a specific tool. It is therefore possible to vary the tool geometry or the cutting conditions in the model to predict the cutting forces, and thus be able to optimize these parameters. If the link between effort and drilling defects are known (ex: bending force → decrease in diameter), it is possible to optimize these parameters to improve the quality of the hole

However, further work is needed to improve the model. As integrate in this model coefficients which evolve in function of the chip thicknesses. And especially which integrates the drilling dynamic, so that the model and the measurements are identical.

6 ACKNOWLEDGEMENTS

7 REFERENCES

[Brinksmeier et al., 2008] Brinksmeier, B; Sascha Fangmann.; Meyer, I; *"Helical milling of CFRP-Titanium layer compounds"*; In: *Prod. Eng. Res. Devel* , pp. 2:277–283; Germany 2008

[Denkena et al., 2008] Denkena, B; Boehnke, D; Dege, J.H.; "Helical milling of CFRP-Titanium layer compounds"; In: *CIRP Journal of Manufacturing Science and Technology*, pp. 64-69; Germany 2008

[Fontaine, 2004] Fontaine, M ; "Modélisation thermomécanique du fraisage de forme et validation expérimentale" Thesis at Metz University ; France ; 2004

[Lorong et al., 2008] Lorong, P; Ali,; "Logiciel explicite en thermomécanique pour la simulation et la formation d'un copeau en usinage"; In: *Mécanique et industrie*, pp. 343-349; Vol3 ; 2002

[Lutze, 2008] S. Lutze. State of the art and expectations for the future of orbital drilling. Thesis at Leuphana University Lüneburg School III 2008

[Merchant, 1945] M.E.Merchant. Mechanics of the metal cutting process, I.Orthogonal cutting, In :*Journal of Applied physics*, vol 16 p318-324 . 1945

[Oxley, 1989] Oxley, P.L.B. Mechanics of metal cutting, Ellis horwood, Chichester, UK, 1989

[Segonds et al, 2006] S.Segonds, Y.Landon, F.Monies, P.Lagarrigue, Method for rapid characterisation of cutting forces in end milling considering runout, in: *International Journal of Machining and Machinability of Materials*, vol. 1 (1), pp. 45-61, 2006.